A&A manuscript no.
(will be inserted by hand later)

Your thesaurus codes are:
6(08.09.2 Algol; 08.12.1; 08.01.2; 08.03.5; 13.25.5)

ASTRONOMY AND ASTROPHYSICS
July 28, 2000

The structure of Algol's corona: a consistent scenario for the X-ray and radio emission

F. Favata[1], G. Micela[2], F. Reale[3], S. Sciortino[2], and J. H. M. M. Schmitt[4]

[1] Astrophysics Division – Space Science Department of ESA, ESTEC, Postbus 299, NL-2200 AG Noordwijk, The Netherlands
[2] Osservatorio Astronomico di Palermo, Piazza del Parlamento 1, I-90134 Palermo, Italy
[3] Dip. Scienze FF. & AA., Sez. Astronomia, Univ. Palermo, Piazza del Parlamento 1, I-90134 Palermo, Italy
[4] Universität Hamburg, Hamburger Sternwarte, Gojenbergsweg 112, D-21029 Hamburg, Germany

Received date 21.03.2000 ; accepted date

Abstract. We present a systematic analysis of the four known large X-ray flares detected to date on the eclipsing binary system Algol, using an approach based on hydrodynamic simulations of decaying flaring loops including sustained heating. This method yields, for the large BeppoSAX Algol flare of Aug. 1997 (where a geometrical estimate of the size of the flaring region is available) a more reliable size than approaches based on the free decay of the flaring loop. For the three flares analyzed here (one observed by EXOSAT, one by GINGA and one by ROSAT) we show that indeed sustained heating is present in all cases, so that the size of the flaring region is always smaller than previously derived. No evidence for the very long loops previously found through quasi-static analysis methods (extending out to several stellar radii) is found. Instead, the flaring corona of Algol is found to be rather compact. By comparing the imaging VLBI observations of the radio corona of Algol with the recent location of the Algol flare seen by BeppoSAX and with with present results, a consistent model of the Algol corona is deduced: the corona is essentially concentrated onto the polar regions of the K star in Algol, with a more compact (smaller than the star) flaring component and a perhaps somewhat more extended (comparable in size to the star) quiescent corona.

Key words: Stars: individual: Algol – late-type – activity – coronae; X-rays: stars

1. Introduction

The study of the decay of large, long-duration stellar flares is one of the key tools for deriving information about the spatial structure of stellar coronae. In the past a variety of techniques has been applied, most of which contain, either explicitly or implicitly, the assumption that the flaring plasma, after an initial more or less impulsive heating event, decays freely by a combination of radiative and conductive cooling. This has often been justified by analogy with impulsive solar events, which are confined to a single loop and which are thought to freely decay after an initial impulsive heating event. These techniques, when applied to intense, long-lasting stellar flares, invariably yield very large flaring loops, with sizes comparable to, or at times much larger than, the star itself. For active binaries these result have prompted the idea of inter-binary loops, with magnetic structures linking the two stars (Uchida & Sakurai 1983). While in the case of the Sun many large flares belong to a different type (the so-called two-ribbon events) in practice the formalism with which they have been described (e.g. Kopp & Poletto 1984) requires many assumptions to be made when applied to spatially unresolved stellar events, so that it has not been possible to use it to obtain well-constrained information about the spatial structuring of stellar coronae.

More recently, a different approach to derive the size of the flaring region from the analysis of the flare decay has been developed by Reale et al. (1997), based on a line of work on the solar corona going back to the classic Rosner et al. (1978), through the studies of e.g. Serio et al. (1991), Sylwester et al. (1993) and Reale et al. (1993). This approach is based on hydrodynamic simulations of decaying loops, and explicitly considers the presence of (decaying) sustained heating also during the decay phase of the flare. Its validity has been shown first on the Sun (Reale et al. 1997), where the availability of Yohkoh images of the flaring events has allowed to compare the decay-derived size with the actual geometrical size, and later on the flare observed on Algol by BeppoSAX (Favata & Schmitt 1999), in which the presence of a total eclipse has allowed to derive the size of the flaring region from geometrical considerations, without any a priori assumption on the characteristics of the flaring region itself. In both cases this approach has proven to have a much better diagnostic power than approaches based on the assumption of free decay. For example, the quasi-static method of van den Oord & Mewe (1989) predicts, for the Algol BeppoSAX flare, much larger loop sizes than actually observed through the flare eclipse.

One of the key results obtained through the application of this approach both on solar and stellar events is the almost ubiquitous presence of sustained heating during the decay of flares.

Send offprint requests to: F. Favata
Correspondence to: ffavata@astro.estec.esa.nl

Sylwester et al. (1993) and Reale et al. (1997) have shown that sustained heating is also present in many compact solar flares, so that their classification as "impulsive events" is actually deceptive. The application of the same approach on stellar flares, on a range of different stellar types – i.e. Reale & Micela (1998), Favata et al. (2000b) and Favata et al. (2000a) on flare stars, Favata & Schmitt (1999) on Algol, Maggio et al. (2000) on AB Dor – has shown that sustained heating is invariably present in all the events studied. In many cases (specially for the large flares) the decay is actually dominated by the time-profile of the heating rather than by the behavior of the flaring loop. An immediate consequence of the presence of sustained heating during the decay phase is that the size of the coronal structures in which the flaring plasma is confined is significantly reduced: previous estimates based on the assumption of free flare decay normally resulted in loops as large or larger than the star itself. Once the presence of sustained heating is accounted for the loops invariably become smaller, with typical sizes $L \lesssim 0.5 R_*$. The smaller inferred loop sizes implies that for very active stars the filling factor of stellar coronae needs not be very high to explain the observed coronal luminosity: in the case of the flare star AD Leo (Favata et al. 2000a) even rather small filling factors (a few percent) can explain the observed coronal luminosity.

Algol is a binary system with of a B8 V primary and a K2 IV secondary (plus a more distant tertiary component, with a period of $\simeq 1.8$ yr and a spectral type A or F). The basic parameters are (Richards 1993) $R_{\rm A} = 2.90\,R_\odot$, $M_{\rm A} = 3.7\,M_\odot$ and $R_{\rm B} = R_* = 3.5\,R_\odot \simeq 2.5 \times 10^{11}$ cm, $M_{\rm B} = 0.81\,M_\odot$, with orbital inclination $i = 81.4$ deg. The orbital period is $\simeq 2.8673$ d. The separation is $14.14\,R_\odot$, or $\simeq 4$ times the radius of the K star.

Algol is a key object for the study of stellar activity: late B stars are not expected to have neither the outer convective envelope required to sustain a dynamo and thus a corona nor the strong, shocked stellar wind which is thought to be responsible for the X-ray emission observed in O and early B stars. Indeed late B stars are in general observed to be X-ray dark (Grillo et al. 1992). The X-ray emission seen in a minority of late-B stars is normally explained as coming from an unseen, low-mass nearby companion. Thus, the high level of magnetic activity observed in Algol is expected to be confined to the K-type secondary, in which the deep convection zone coupled with the rapid rotation will sustain a vigorous dynamo. Therefore complex, inter-binary magnetic loops are unlikely to be present, and the corona will likely have the same structure as the one of a single star with comparable levels of activity. The high activity level and proximity to Earth of Algol allow for high S/N spectroscopic observations to be performed. The presence of the X-ray-dark B-type primary which eclipses the active K-type secondary has allowed to obtain, for the first time, a geometrical estimate of the size of a flaring structure on a star other than the Sun (Schmitt & Favata 1999). Its high radio luminosity (Mutel et al. 1998) allows detailed VLBI imaging, making a comparison of the radio and X-ray corona possible. Also, the high frequency of large flares on the active K-type secondary makes it a target of choice: indeed by now a significant database of X-ray observations of Algol exists, and four large flaring events have been observed (by EXOSAT, GINGA, ROSAT and BeppoSAX), so that the frequency of (large) flares can be estimated as approximately one every two orbits, i.e. $\simeq 5$ d (Ottmann & Schmitt 1994). The orbital period is 2.87 d, and each optical eclipse lasts approximately 10 hr.

In the present paper we aim to characterize the corona of Algol by studying all known large X-ray flares in a homogeneous way, using the approach based on hydrodynamic simulations of the decaying loops of Reale et al. (1997), together with the published studies on the radio corona of Algol and on its quiescent X-ray emission. Through this systematic approach we obtain a consistent picture of Algol's corona, and verify that the conclusions obtained by Schmitt & Favata (1999) and Favata & Schmitt (1999) from the analysis of the BeppoSAX flare have a far more general applicability. The flaring events studied here have been analyzed in the past with a consistent methodology, the so-called quasi-static approach, which van den Oord & Mewe (1989) originally applied to the EXOSAT Algol flare. The GINGA flare was analyzed by Stern et al. (1992), while the ROSAT one was studied by Ottmann & Schmitt (1996), in both cases using the same method as used for the EXOSAT event. In all cases the size of the coronal structure responsible for the flaring event was found to be larger than the stellar radius (see Table 1). Although the van den Oord & Mewe (1989) approach considers the possibility of heating during the decay phase, the fit to the EXOSAT and ROSAT events did not require sustained heating (which, as we show in the following, is actually present). For the GINGA event the lack of sustained heating was actually assumed, rather than derived from the data.

The present paper is so structured: Sect. 2.1, 2.2 and 2.3 contain the analysis of the Algol flares observed by EXOSAT, GINGA and ROSAT, respectively; the essential results from the BeppoSAX flare are recalled in Sect. 2.4; Sect. 3 discusses the available evidence from radio observations, comparing it with the information from X-ray observations, while Sect. 4 presents a consistent scenario for Algol's corona explaining both the X-ray and radio observations. A brief Appendix contains the detailed prescriptions for application of the Reale et al. (1997) method to flaring events observed with the EXOSAT ME and the GINGA LAC instruments, as well as for events observed with the ROSAT PSPC which have sufficient statistics for the flare decay to be resolved into individual spectra.

2. Analysis of the flaring events

2.1. The EXOSAT flare

EXOSAT observed Algol on 18 and 19 August 1983, for a total of $\simeq$ 33 hr. During the observation with the Medium Energy (ME) detector a significant flare was detected, which has been analyzed in detail by van den Oord & Mewe (1989). The ME detector had a bandpass of $\simeq$ 1 to $\simeq$ 15 keV and an energy resolution of $\simeq$ 20% at 6.7 keV. The spectral fitting to the ME spectra gives a flare peak temperature $T_{\rm obs} = 78$ MK

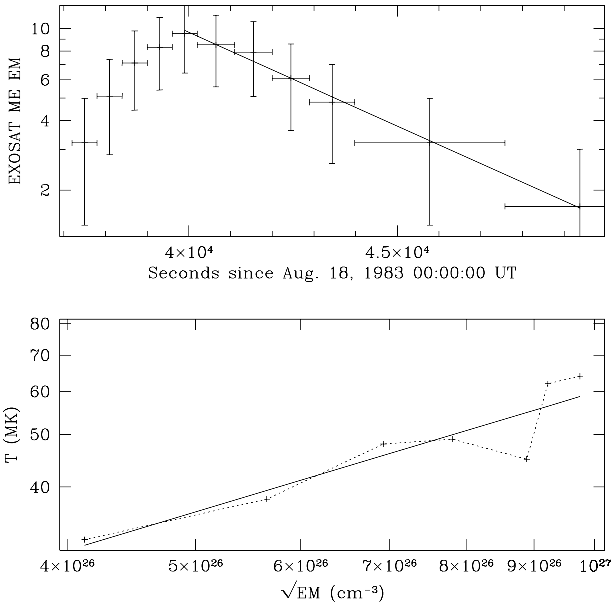

Fig. 1. The evolution of the EXOSAT Algol flare. The top panel shows the evolution of the emission measure during the flare, together with the best-fit exponential decay, while the bottom panel shows the evolution of the flare's decay in the $\log T$ vs. $\log n$ plane. The dotted line connects the points in their temporal order, while the solid line is the best fit to the decay.

and a peak emission measure $EM = 0.95 \times 10^{54}$ cm^{-3}. The main result of the van den Oord & Mewe (1989) analysis is that the flare is found to satisfy the condition for quasi-static decay, with no evidence for prolonged heating (i.e. it is seen as an "impulsive" event), with a resulting loop length $L = 16 \times 10^{10}$ cm, or $L \simeq 0.6\, R_*$.

We have analyzed the same flare with the Reale et al. (1997) approach, using the temporal evolution of the temperature and emission measure as determined by van den Oord & Mewe (1989). The results are shown in Fig. 1: the effective decay time of the X-ray count rate[1] is $\tau_{\rm LC} = 5.3\ [5.0,\ 5.5]$ ks[2], while $\zeta = 0.73 \pm 0.15$. Application of Eq. (A4) yields $\tau_{\rm LC}/\tau_{\rm th} = F(\zeta) = 2.4\ [1.9,\ 3.6]$, showing that the thermodynamic decay time $\tau_{\rm th}$ of the loop is significantly shorter than the observed decay time $\tau_{\rm LC}$, and therefore that sustained heating is present during the decay phase. The lack of sustained heating was, in van den Oord & Mewe (1989), a result obtained by fitting the data, i.e. was not assumed; thus, the assumptions of the quasi-static heating method may not be appropriate for real stellar flares, and its diagnostic power for the presence of decay-phase heating is likely to be limited. The thermodynamic decay time of the flaring loop is only $\tau_{\rm th} = 2.3$ ks, while the maximum temperature (from Eq. (A5)) is $T_{\rm max} \simeq 151$ MK and the resulting length of the flaring region is $L = 7.5\ [4.8,\ 9.8] \times 10^{10}$ cm, or $L \simeq 0.3\ [0.2,\ 0.4]\ R_*$.

[1] For the EXOSAT ME data no count rates were reported by the original authors, only the emission measures. We have verified that in the range of plasma temperatures of interest here the emission measure accurately tracks the count rate in the ME passband, and thus that it can be used as proxy for it without introducing any additional significant uncertainty.

[2] Here, as in the following, the numbers within square parentheses indicate the 1 σ range for the quantity.

2.2. The GINGA flare

Algol was observed by GINGA with the LAC (Large Area Counter) instrument in January 1989, covering approx. 22 hr elapsed time. The LAC has a passband of 1.2–37 keV, with an energy resolution of 18% FWHM at 5.9 keV. The observation (analyzed by Stern et al. 1992) contains two flares, the largest of which (starting at about Jan. 14 02:00 UT) features a factor of $\simeq 4$ increase in count rate in the LAC.

Stern et al. (1992) have studied the large flare in detail, deriving the temporal evolution of the spectral parameters and analyzing the decay phase to obtain the physical parameters of the flaring regions using the quasi-static approach previously used on the EXOSAT Algol flare by van den Oord & Mewe (1989). The peak temperature of the event is 67 ± 12 MK, the peak emission measure 1.34×10^{54} cm^{-3}, and the e-folding time of the X-ray luminosity 20.0 ks. The EXOSAT analysis has been scaled by Stern et al. (1992) to derive (under the same assumptions) a loop length of $\simeq 6 \times 10^{11}$ cm ($2.5\ R_{\rm K}$) and a density $n \simeq 5 \times 10^{10}$ cm^{-3}. Later, Stern (1996) plotted the evolution of the same event in the $\log T$ vs. $\log \sqrt{EM}$, without however drawing any specific conclusions from it.

Our analysis of the GINGA event within the sustained heating framework uses the temperature, count rate and emission measure values published by Stern et al. (1992). The evolution of the GINGA flare is shown in Fig. 2, where both the light-curve and the $\log T$ vs. $\log \sqrt{EM}$ diagrams are shown, together with the best fits to the decay phase. The quiescent emission count rate (18 cts s^{-1}) determined during the same observation has been subtracted from the plotted light-curve. The light-curve e-folding time is $19.8\ [18.8,\ 20.9]$ ks, while the slope of the decay in the $\log T$ vs. $\log \sqrt{EM}$ diagram is $\zeta = 0.44 \pm 0.1$, with $F(\zeta) = 4.2\ [3.6,\ 4.8]$ (derived through Eq. (A6)). Such large value of $F(\zeta)$ implies very strong sustained heating, so that the light-curve is in this case dominated by the temporal evolution of the plasma heating rather than by the natural decay of the flaring loop. The peak temperature of the flaring loop is (from the observed peak temperature $T_{\rm obs} = 67$ MK and Eq. (A7)) $T_{\rm max} = 104$ MK. The resulting loop length is (Eq. (A1)) $L = 1.3\ [1.1,\ 1.6] \times 10^{11}$ cm ($0.5\ [0.4,\ 0.6]\ R_{\rm K}$); the significant difference with the result of Stern et al. (1992) is due to the dominating influence of sustained heating.

2.3. The ROSAT PSPC flare

A long observation of Algol was performed with the ROSAT PSPC detector in August 1992, spanning 2.4 orbits of the system ($\simeq 600$ ks elapsed time), although with an irregular sampling. During the observation a large flare (with a $\simeq 10\ \times$ increase in count rate) was observed. The event has been ana-

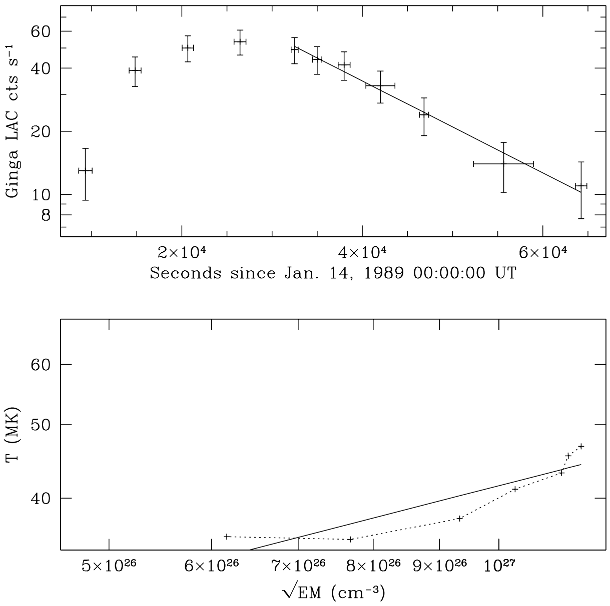

Fig. 2. The evolution of the GINGA Algol flare. The top panel shows the (background-subtracted) flare's light curve, together with the best-fit exponential decay, while the bottom panel shows the evolution of the flare's decay in the $\log T$ vs. $\log n$ plane. The dotted line connects the points in their temporal order, while the solid line is the best fit to the decay.

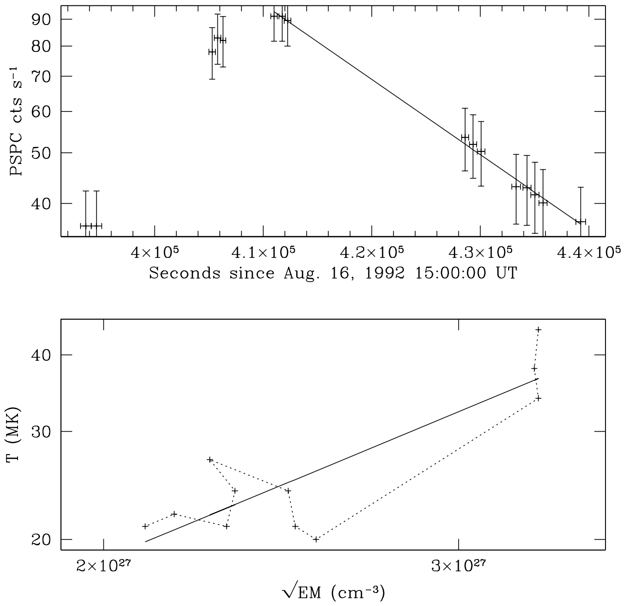

Fig. 3. The evolution of the PSPC Algol flare. The top panel shows the (background-subtracted) flare's light curve, together with the best-fit exponential decay, while the bottom panel shows the evolution of the flare's decay in the $\log T$ vs. $\log n$ plane. The dotted line connects the points in their temporal order, while the solid line is the best fit to the decay.

lyzed in detail by Ottmann & Schmitt (1996), using the quasi-static framework. The decay time scale reported by Ottmann & Schmitt (1996) is $\tau_{\rm LC} = 30.4$ ks, and the peak temperature determined through the PSPC is $T = 44$ MK. The quasi-static fit performed by Ottmann & Schmitt (1996) includes (as for the EXOSAT event) allowance for the presence of heating during the decay phase; however the best-fit value of the heating function is zero, so that no sustained heating is evident from the quasi-static analysis. The derived loop lenght is $L = 5.0 \times 10^{11}$ cm, or $L \simeq 2.0\ R_*$. The derived density is $n \simeq 5 \times 10^{11}$ cm^{-3}.

We have analyzed the Algol PSPC flare, as shown in Fig. 3, adopting the spectral parameters of Ottmann & Schmitt (1996). The top panel of Fig. 3 shows the light curve (together with the best-fit exponential decay, which has $\tau_{\rm LC} = 30.2 \pm 0.5$ ks), while the bottom panel shows the flare decay in the $\log T$ vs. $\log n$ plane. The decay's slope ($\zeta = 1.37 \pm 0.28$) implies (through Eq. (A8)) a ratio $\tau_{\rm LC}/\tau_{\rm th} = F(\zeta) = 2.6\ [2.4,\ 3.0]$, thus showing that significant sustained heating is present, again though the quasi-static analysis (even in its full blown formalism, as used by Ottmann & Schmitt 1996) explicit derives its absence (a situation similar to the one of the EXOSAT flare, Sect. 2.1). The flare's peak temperature (scaled from the maximum measured temperature of 44 MK through Eq. (A9)) is $T_{\rm max} \simeq 100$ MK. Through Eq. (A1) the derived loop length is $L = 31\ [28,\ 33] \times 10^{10}$ cm, or $L \simeq 1.2\ [1.1,\ 1.3]\ R_*$.

The temporal coverage of the PSPC flare is rather sparse, in particular the first phase of the decay (immediately following the three points at $\simeq$ 90 cts s^{-1} in Fig. 3) has not been observed. This introduces a large potential systematic error in the determination of the flare's physical parameters. In particular the decay time of the light curve could be over-estimated: if the flare would have been "hovering" near the peak, during the observing gap, the actual decay would be faster than observed, and thus the flaring loop smaller than derived here. Thus, in this case the derived length should be considered as an upper limit to the actual size of the loop.

2.4. The BeppoSAX flare

The large flare observed by BeppoSAX on Algol in Aug. 1997 was already analyzed in detail, using the Reale et al. (1997) approach, by Favata & Schmitt (1999). Due to the complex evolution of the event (with the temperature rising again midway through the decay) the hydrodynamic modeling yields a wide range of possible values for the loop's length, comprised between 47 and 120×10^{10} cm (1.8 and 4.8 R_*), while the observed eclipse puts an upper limit of 24×10^{10} cm (0.9 R_*) on the loop size (on the assumption of a simple loop geometry, as the actual eclipse constraint is on the maximum height of the flaring region above the stellar surface, which is $H \leq 15 \times 10^{10}$ cm, or $H \leq 0.6\ R_*$). Thus, the loop is smaller than the stellar size, and even the hydrodynamic simulation modeling is, if anything, likely to somewhat overestimate the loop's size. Additionally, the eclipse timing (Schmitt & Favata

1999) shows that the event is located above the southern polar cap of the K-type secondary.

2.5. *Plasma density and scale height*

No direct estimate of the plasma density is produced by the approach used here to analyze the flares. However, a simple estimate can be obtained by dividing the emission measure by the loop volume, i.e.

$$n = \sqrt{\frac{EM}{2\pi L^3 \beta^2}} \tag{1}$$

where β is the loop's aspect ratio. In the solar case typically $\beta \simeq 0.1$, and this value has often been used (assumed) also for stellar flares. However, recent analyses (Favata et al. 2000a; Maggio et al. 2000) of stellar flares with the same approach used here point to a larger value for stellar flaring loops, with $\beta \simeq 0.3$ giving a better agreement between the pressure so derived and the pressure obtained by applying the scaling laws of Rosner et al. (1978) to the observed loop sizes and temperatures. We have therefore used both $\beta = 0.1$ and $\beta = 0.3$ in computing an estimate for the loop's density, as reported in Table 1. For all flares analyzed here, the plasma densities are typically $\leq 10^{11}$ cm^{-3}.

Also, all derived loop sizes are small in comparison with the pressure scale height[3] in the corona of the active star in Algol, which is greater than 5×10^{12} cm for all the events discussed here, thus justifying the initial assumption done in the modeling that the flaring loops are isobaric.

3. Comparison with the radio corona of Algol

VLBI radio techniques have sufficient resolution to allow direct "imaging" of the radio-bright component of the Algol corona, although the uncertainties in the relative astrometry do not allow for accurate positioning of the photosphere of the two stars onto the radio map. Mutel et al. (1998) have recently studied Algol with a long time series (along more than 1 yr) of VLBA observations, finding frequent large flares superimposed on a relatively constant quiescent emission level. The map of the radio corona shows the presence of two lobes, aligned with the poles of the system, and plausibly positioned on the poles of the active K star in Algol. The regions from which the quiescent emission originates are resolved in the radio images, and are larger than the star itself. No evidence for orbital modulation of the (quiescent) radio emission is seen, thus implying that the emitting plasma is largely located outside of the orbital plane of the system. The flaring emission comes from the same region as the quiescent one, but is not spatially resolved in the VLBA observations (i.e. the emitting regions are smaller than the radio beam), and is comparable to or smaller in size than the star. Mutel et al. (1998) thus model the flaring regions as co-located with the ones responsible for the quiescent emission, but significantly more compact (see their Fig. 13). No radio emission is identified from regions around the star's equator, nor from the inter-binary region. The radio emission coming from two lobes is polarized, with opposite signs, implying the presence of magnetic fields of opposite polarity, which Mutel et al. (1998) interpret as possibly coming from a large-scale bipolar magnetic field.

How does the X-ray corona compare with the radio one? The evidence from the existing X-ray observations of Algol is that the level of orbital modulation of the quiescent X-ray emission is small, if not, at times, negligible: the ROSAT and ASCA observations show a $\simeq 15\%$ decrease in the X-ray emission at secondary minimum (Ottmann 1994; Antunes et al. 1994), while no orbital modulation of the quiescent emission is seen in the EXOSAT observation (White et al. 1986). At the same time, the BeppoSAX flare undergoes a total eclipse, while the EXOSAT, GINGA and PSPC flares (the ones analyzed in the present paper) do not show any evidence of eclipses. The very shallow orbital modulation of the quiescent emission has been interpreted (e.g. White et al. 1986) as implying that the X-ray emitting region is so extended that the companion star can only eclipse a small fraction of it at any given time (thus as large or larger than the inter-binary separation). However, an alternative explanation (which Mutel et al. 1998 use also for the radio emission) is that the coronal plasma is confined largely to regions above the polar caps of the active star. The emitting region is thus not eclipsed (except for a small volume close to the K star's polar surface) in a high-inclination binary such as Algol. The seat of the quiescent emission must thus be more extended than the region being eclipsed by the primary during secondary eclipse, but not much more. This implies that it must extend above $H \simeq 0.6\ R_*$, perhaps to a size comparable to the size of the region postulated by Mutel et al. (1998) for the quiescent *radio* corona. The BeppoSAX flare has been shown to be located on the South pole of the Algol K star, and to be more compact than $H \simeq 0.6\ R_*$ – thus fully compatible with the type of region postulated by Mutel et al. (1998) for the flaring *radio* corona. The other three X-ray flares have not been eclipsed and thus their location on the star cannot be established; however their size as derived here is also compact and thus compatible with the same picture.

The X-ray and radio data can thus be explained within the same scenario: the corona is essentially polar and located on the K star in Algol (with no influence from the B star except for the tidally induced rotation), with a compact flaring component (smaller than the star) and a more extended quiescent corona, as large or somewhat larger than the star itself. The latter shows little if any rotational modulation as the B star can only occult a small fraction of the southern lobe.

4. Discussion

The physical parameters derived from the analysis of the decay of the four major X-ray flares observed to date on Al-

[3] defined as $H = 2kT/\mu g$, where T is the plasma temperature in the (flaring) loop, μ the molecular weight of the plasma and g the star's surface gravity.

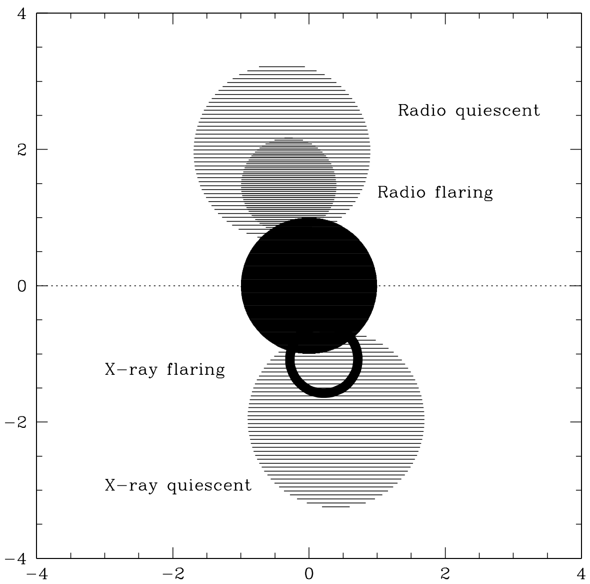

Fig. 4. A schematic view of the corona of Algol. The central black disk represents the K star, while the two lobes on the northern pole represent the location of the quiescent (larger lobe) and flaring (smaller lobe) radio corona, from Mutel et al. (1998). On the southern pole a loop of the size implied by the GINGA flare is shown. The larger lobe represents the location of the quiescent X-ray corona.

gol are listed in Table 1, in which both the size derived by a quasi-static analysis and the one derived in the present paper through a hydrodynamic modeling approach are reported (for the BeppoSAX flare the eclipse-derived size is actually smaller, at $L \simeq 0.9\ R_*$). In all cases, the size derived from the hydrodynamic modeling is significantly smaller than the quasi-static derived size, and also smaller (or comparable to) than the stellar size. The presence, in the case of the BeppoSAX flare, of a total eclipse has allowed to independently derive a size of the flaring region and thus to test the various modeling approaches: the hydrodynamic modeling approach used here is significantly more reliable in deriving the size of the emitting region, and, if anything, it will over-predict (rather than under-predict) the size so that the actual loop sizes are unlikely to be larger than discussed here.

As discussed in Sect. 3, a consistent scenario can be derived for the Algol corona for both the X-ray emitting and the radio-emitting components. A schematic view of the two is shown in Fig. 4; the resulting coronal geometry is very different from the solar one, and is not a simple "scaled-up" version of it: the corona is confined to the polar regions of the star (with no evidence of significant low-latitude active regions), and the flaring corona is significantly more compact than the quiescent one. The radio polarization also argues for a coherent large-scale magnetic field (i.e. a near-bipolar configuration), while the X-ray observations do not allow this distinction to be made. Again, this magnetic field configuration would be very different from the solar one. It is not straightforward to understand how polar coronal loops fit in this picture, i.e. whether real polar loop-like structures are present, such as the one sketched in Fig. 4, or whether for example the active plasma is confined at the foot of much larger loop-like structures which follow the bipolar field structure (i.e. connect the two poles).

Evidence for the polar location of active regions is becoming available on different types of stars with very high activity levels: long-lasting flares show no evidence of significant auto-eclipse even when their duration is comparable to the stellar orbital period, e.g. the EV Lac (a flare star) PSPC event reported by Schmitt (1994), which lasted for more than one rotational period of the star, or the AB Dor (a near-ZAMS solar-type star) BeppoSAX events reported by Maggio et al. (2000), which have a duration comparable to the stellar rotational period. The lack of self-eclipses of the quiescent emission on RS CVn-type binaries (see Schmitt 1998 for a review) is also compatible with an Algol-like scenario, in which activity is concentrated on the polar caps of both components – thus resulting in very small levels of rotational modulation. Indeed Mutel et al. (1998) note that the radio emission characteristics of the active binary AR Lac are very similar to Algol's – pointing to a similarly structured corona, even though both stars are likely to have significant activity in AR Lac. Additional evidence comes also from the long EUVE observations of the contact binary 44 Boo of Brickhouse & Dupree (1998): the level of rotational modulation is very small, and with a period slightly smaller than the orbital period of the system. The density is also very high ($n \simeq 2 \times 10^{13}$ cm^{-3}). Brickhouse & Dupree (1998) model this as emission coming from a compact region located at high latitude ($>$ 72 deg), thus again a largely polar corona. The difference between the observed modulation period and the orbital period is interpreted as being due to the presence of differential rotation. A possible scenario is thus that the coronal geometry of very active stars – independently from their type, i.e. whether they are single flare stars, or active binaries, or very young solar-type dwarfs – entails in general the presence of active polar regions, with only small amounts of low-latitude coronal emission.

Acknowledgements. We would like to thank Bob Stern for the useful discussion on his analysis of the GINGA flare, and Giovanni Peres for the many discussion on the solar-stellar paradigm. We also thank an anonymous referee for his/her very accurate reading of the manuscript and for his/her helpful comments which helped improve the paper. FR, GM and SS acknowledge the partial support of ASI and MURST.

References

Antunes A., Nagase F., White N. E. 1994, ApJ, 436, L83
Brickhouse N. S., Dupree A. K. 1998, ApJ, 502, 918
Favata F., Micela G., Reale F. 2000a, A&A, 354, 1021
Favata F., Reale F., Micela G. et al. 2000b, A&A, 353, 987
Favata F., Schmitt J. H. M. M. 1999, A&A, 350, 900
Grillo F., Sciortino S., Micela G., Vaiana G. S., Harnden F. R. 1992, ApJS, 81, 795
Kopp R. A., Poletto G. 1984, Sol. Phys., 93, 351

Table 1. A comparison of the physical parameters derived for different flares on Algol from the GINGA, EXOSAT, ROSAT and BeppoSAX flares. T_p: observed maximum temperature during the flare. T_d: observed temperature at the beginning of the flare's decay (i.e. at the peak of the flare's emission measure or count rate). EM: peak emission measure of the flare. τ_LC: $1/e$ decay time of the flare's light curve (or emission measure), as determined here. n^QS: density of the flaring plasma at the beginning of the decay phase as determined by the quasi-static analyses in the original papers. $F(\zeta)$: ratio between the observed luminosity decay time τ_LC and thermodynamic free decay time of the loop τ_th. L^QS: length of the flaring loop determined by the quasi-static analyses of the original papers: L^HY: length of the flaring loop determined here. n: density derived through the observed peak emission measure EM and the loop length L^HY; the first value assumes loops with aspect ratios $\beta = 0.1$ while the second one assumes $\beta = 0.3$. Numerical subscripts indicate the power of 10 by which the relevant quantity has been scaled.

Instr.	T_p MK	T_d MK	EM_{54} cm^{-3}	τ_LC ks	n_{10}^QS cm^{-3}	$F(\zeta)$	τ_th ks	L_{10}^QS cm	L^QS R_*	L_{10}^HY cm	L^HY R_*	n_{10} cm^{-3}
EXOSAT	78	64	0.95	5.3	26	2.4	2.3	16	0.6	7.5	0.3 [0.2 0.4]	6.3 – 19
GINGA	67	47	1.34	19.8	5	4.2	4.7	60	2.4	13	0.5 [0.4 0.6]	3.2 – 9.9
ROSAT	44	44	10.8	30.2	50	2.6	11.4	50	2.0	31	1.2 [1.1 1.3]	2.5 – 7.6
SAX	142	98	13.3	49.6	9	2.4	20.1	174	7.0	82	3.3 [1.9 4.7]	2.0 – 6.0

Maggio A., Pallavicini R., Reale F., Tagliaferri G. 2000, A&A, in press,

Mutel R. L., Molnar L. A., Waltman E. B., Ghigo F. D. 1998, ApJ, 507, 371

Ottmann R. 1994, A&A, 286, L27

Ottmann R., Schmitt J. H. M. M. 1994, A&A, 283, 871

Ottmann R., Schmitt J. H. M. M. 1996, A&A, 307, 813

Reale F., Betta R., Peres G., Serio S., McTiernan J. 1997, A&A, 325, 782

Reale F., Micela G. 1998, A&A, 334, 1028

Reale F., Serio S., Peres G. 1993, A&A, 272, 486

Richards M. T. 1993, ApJS, 86, 255

Rosner R., Tucker W. H., Vaiana G. S. 1978, ApJ, 220, 643

Schmitt J. H. M. M. 1994, ApJS, 90, 735

Schmitt J. H. M. M. 1998, in R. A. Donahue, J. A. Bookbinder (eds.), Cool Stars, Stellar Systems and the Sun, Vol. 154 of *ASP Conference Series*, ASP, San Francisco, 463

Schmitt J. H. M. M., Favata F. 1999, Nat, 401, 44

Serio S., Reale F., Jakimiec J., Sylwester B., Sylwester J. 1991, A&A, 241, 197

Stern R. A. 1996, in IAU Colloq. 153: Magnetodynamic Phenomena in the Solar Atmosphere - Prototypes of Stellar Magnetic Activity, 83

Stern R. A., Uchida Y., Tsuneta S., Nagase F. 1992, ApJ, 400, 321

Sylwester B., Sylwester J., Serio S. et al. 1993, A&A, 267, 586

Uchida Y., Sakurai T. 1983, in IAU Colloq. 71: Activity in Red-Dwarf Stars, p. 629

van den Oord G. H. J., Mewe R. 1989, A&A, 213, 245

White N. E., Culhane J. L., Parmar A. N. 1986, ApJ, 301, 262

Appendix A: Calibration of the flare analysis method

The flare analysis method of Reale et al. (1997) needs to be separately calibrated for each detector, due the different spectral bandpass and resolution. In the present Appendix we present the calibration for the EXOSAT ME and for the GINGA LAC detectors, as well as for the ROSAT PSPC when flares can be broken into temporal segments with sufficient statistics as to be individually fit (an alternate approach optimized for low-statistics PSPC flares is discussed by Reale & Micela 1998). The details of the method used here are discussed in Reale et al. (1997).

For each individual detector, the ratio between the observed decay time of the light curve τ_LC and the "natural" thermodynamic cooling time of the loop without additional heating τ_th (Serio et al. 1991) needs to be calibrated as a function of the slope ζ of the flare decay in the $\log T$ vs. $\log \sqrt{EM}$ plane. This allows to derive τ_th from the observed quantities τ_LC and ζ and thus to derive the loop length from the relationship

$$\tau_\mathrm{th} = \frac{\alpha L}{\sqrt{T_\mathrm{max}}} \tag{A1}$$

where $\alpha = 3.7\ 10^{-4}\ \mathrm{cm^{-1}s^{-1}K^{1/2}}$ and T_max is the actual peak temperature of the plasma in the flaring loop, which in turn needs to be calibrated as a function of the maximum temperature determined through spectral fitting of the observed flare spectrum T_obs. For each instrument thus the two functions that need to be determined are

$$F(\zeta) = \frac{\tau_\mathrm{LC}}{\tau_\mathrm{th}} \tag{A2}$$

and

$$T_\mathrm{max} = G(T_\mathrm{obs}) \tag{A3}$$

with T in K as in all the following equations.

In general, $F(\zeta) > 1$ implies that sustained heating is present during the decay of the flare, and thus that the assumption of free decay of the flare will lead to overestimate the size of the flaring region, by a factor roughly comparable to $F(\zeta)$ itself. In practice this means a shallow decay in the $\log T$ vs. $\log \sqrt{EM}$ plane, i.e. the temperature of the flaring plasma decays more slowly than its emission measure. When $F(\zeta) \simeq 1$, the size of the flaring region estimated assuming free decay will be very similar to the size estimated with the present approach.

Using temperatures and emission measures determined by spectral fitting to EXOSAT ME data the function $F(\zeta)$ is

$$\tau_{\rm LC}/\tau_{\rm th} = F(\zeta) = \frac{1.3}{\zeta/0.4 - 1.0} + 0.8 \qquad 0.4 \le \zeta \le 1.8 \tag{A4}$$

where the range of validity for the relationship is also given. The peak temperature is given by

$$T_{\rm max} = 0.231 \times T_{\rm obs}^{1.117} \tag{A5}$$

For the GINGA LAC detector the corresponding relationships are

$$\tau_{\rm LC}/\tau_{\rm th} = F(\zeta) = c_a e^{-\zeta/\zeta_a} + q_a \qquad 0.43 \le \zeta \le 1.6 \tag{A6}$$

with $c_a = 7.65$, $\zeta_a = 0.72$, $q_a = 0.0$. The actual peak temperature $T_{\rm max}$ of the plasma in the flaring loop is related to the observed peak temperature of the flare through

$$T_{\rm max} = 0.347 \times T_{\rm obs}^{1.083} \tag{A7}$$

Finally, if ROSAT PSPC-derived temperatures and emission measures are used,

$$\tau_{LC}/\tau_{th} = F(\zeta) = \frac{3.67}{\zeta/0.3 - 1.0} + 1.61 \qquad 0.4 \le \zeta \le 1.7 \tag{A8}$$

while

$$T_{\rm max} = 0.173 \times T_{\rm obs}^{1.163} \tag{A9}$$